PHYSICAL REVIEW E **78**, 055301(R) (2008)

Brownian demixing and wall effects in sedimenting suspensions of orientable particles

Brendan D. Hoffman[1] and Eric S. G. Shaqfeh[1,2,*]
[1]*Department of Chemical Engineering, Stanford University, Stanford, California 94035, USA*
[2]*Department of Mechanical Engineering, Stanford University, Stanford, California 94305, USA*
(Received 14 July 2008; published 3 November 2008)

We describe the *Brownian demixing* of sedimenting suspensions, a recently discovered phenomenon in which increases in the thermal energy can destabilize a system of orientable particles subjected to a torque to fluctuations in concentration. Through use of Brownian dynamics simulation and a mean-field analysis, we demonstrate that demixing occurs in a model system composed of slender rigid rods sedimenting between no-slip walls. Additionally, we describe the effects of wall separation distance on suspension stability.

DOI: 10.1103/PhysRevE.78.055301 PACS number(s): 47.57.ef, 47.57.J−

The recent demand for microfluidic technologies for biomedical purposes, such as bioassays using nano-barcodes or the processing of complex fluids for medical diagnostics, has led to an interest in the behavior of Brownian suspensions in confined geometries [1–4]. Often a suspension's microstructure is determined by a device's operating environment, which may include the presence of externally applied fields, concentration gradients driving "swimming" particles, or a mean flow in laboratory-on-a-chip applications, to name a few. The suspension microstructure directly determines its dynamic properties; one such property which may affect device performance is the instability of sedimenting orientable particles to density fluctuations. As particles sediment, hydrodynamic interactions between regions of varying density result in a net migration of particles into the denser region via orientational changes. The instability is characterized by the formation of particle streamers which settle, on average, faster than the maximum settling velocity of an isolated particle in Stokes flow. This Rapid Communication will examine the instability formation as it applies to rigid slender rods; it should be noted, however, that it has been demonstrated for orientable and deformable particles in general [5].

Experiments [6] have confirmed the existence of the instability, and theoretical models have been reasonably successful at predicting its formation [7–9]. When no particle torques are present, the stability of a suspension of sedimenting rigid rods of length $2L$ is determined by a gravitational Peclet number,

$$\mathrm{Pe}_g = \frac{|\mathbf{F}_g|L}{k_B T}, \tag{1}$$

which relates a particle's net gravitational force $|\mathbf{F}_g|$ to the thermal energy. At $\mathrm{Pe} \sim O(1)$, the hydrodynamic torques driven by gravity are approximately balanced by the Brownian forces which randomize particle orientation. Thus, at sufficiently low Peclet numbers, the tendency of thermal motion to restore the suspension's isotropic orientation offsets the driving force of the instability formation, stabilizing the suspension. Additionally, center-of-mass diffusive motion tends to disperse regions of high concentrations, disrupting density perturbations. Brownian stabilization of unbound suspensions was recently analyzed in detail by Hoffman and Shaqfeh [7], where they found that the longest wavelength concentration fluctuations are the least stable.

Hoffman and Shaqfeh also examined the effect of Brownian motion on the stability of polarizable rod suspensions in electric fields. In an electrolyte, the rod polarization results in the formation of a double layer which, when coupled with the resulting disturbance flow, drives a slip velocity which forces the particle to orient with the field, a phenomenon known as induced-charge electrophoresis (ICEP) [1]. Previous work by Saintillan *et al.* [10] demonstrated that for non-Brownian suspensions, particles undergoing ICEP in strong electric fields are more stable than those without field effects. This is due to a preferential particle alignment with the electric field, which, much like the effects of Brownian motion, allows the particles to resist the hydrodynamic torque caused by density fluctuations. Somewhat counterintuitively, Hoffman and Shaqfeh [7] found a region of Peclet number at which, keeping the strength of the electric field relative to gravity constant, the effects of increased Brownian motion were to *destabilize* the suspension.

In this Rapid Communication, we show that this phenomenon of *Brownian demixing* is universal in suspension mechanics and will occur whenever sedimentation occurs in the presence of a particle torque $\hat{\mathbf{B}}$. Example systems include, in addition to ICEP, the alignment of particles in magnetic or electric fields, self-locomoting bacteria that seek preferential alignment, or particles sedimenting against a shear flow. When no Brownian motion is present, the stability of a suspension will be governed by a dimensionless torque F, which describes the balance between the externally imposed alignment and gravity, which drives the instability: $F = |\hat{\mathbf{B}}|/(|\mathbf{F}_g|L)$. As the particle size becomes smaller and thermal effects become increasingly important, both Pe_g and/or F will mutually determine the suspension stability, resulting in a rich phase behavior.

Brownian demixing occurs in a transition region between a stable, aligned suspension ($\mathrm{Pe}_g \to \infty$) and a stable, isotropically oriented suspension ($\mathrm{Pe}_g \to 0$) as the Peclet number is decreased at constant F. The essential feature of this phenomenon is that the increased effects of Brownian motion alter the orientation distribution of suspended particles via a random torque, allowing particles to sample orientations away from the aligned state which promote instability through gravity driven hydrodynamic interactions. In other

*esgs@stanford.edu

words, the Brownian motion sufficiently disrupts the aligning effect of the torque, driving the orientation distribution into an "intermediate" state between isotropic and aligned that is more unstable to concentration perturbations than either of the two extreme cases. As the Peclet number approaches 0, stability is restored through a complete randomization of particle orientation, dominating both gravitational and external torque effects. There has been some evidence in a paper by Saintillan *et al.* [9] that certain orientation distributions calculated from Onsager theory yield a relative maximum in instability growth rate vs alignment parameter. Their analysis, however, only applied to the *initial* orientation distribution and neglected the effects of Brownian motion.

Wall effects become particularly important in microfluidic devices, as the channel width is often only a few particle lengths. To study Brownian demixing in confined channels, we have examined the effects of Brownian motion on the stability of a suspension of sedimenting slender fibers in a channel of width h (measured in particle $1/2$ lengths, with the suspension periodic in the remaining two dimensions) through a mean-field analysis and Brownian dynamics simulation (BDS), described below.

The kinematic equations describing the motion of slender particles with orientation vector $\mathbf{p}$ suspended in a fluid of viscosity μ and subject to a body force $\mathbf{F}$ are given to $O[1/\ln(2A)]$ as

$$\dot{\mathbf{x}} = \frac{1}{2L}\int_{-L}^{L} \mathbf{u} ds + \frac{\ln(2A)}{8\pi\mu L}(\mathbf{I}+\mathbf{pp})\cdot\mathbf{F}, \tag{2}$$

$$\dot{\mathbf{p}} = \frac{3}{2L^3}(\mathbf{I}-\mathbf{pp})\int_{-L}^{L} \mathbf{u} s ds - \frac{3\ln(2A)}{8\pi\mu L^3}\mathbf{p}\times\mathbf{T}, \tag{3}$$

where $\mathbf{u}$ is the disturbance velocity caused by all other particles in the suspension (or walls).

In the mean-field theory, we represent the suspension by a particle concentration field $c(\mathbf{x},\mathbf{p})$ and evaluate its stability using a linear stability analysis of the particle conservation equation,

$$\frac{\partial c}{\partial t} + \nabla_{\mathbf{p}}\cdot(\dot{\mathbf{p}}c) + \nabla_{\mathbf{x}}\cdot(\dot{\mathbf{x}}c) - d_r\nabla_{\mathbf{p}}^2 c - \nabla_{\mathbf{x}}\cdot\mathbf{D}\cdot\nabla_{\mathbf{x}}c = 0, \tag{4}$$

where $\mathbf{D}$ and d_r are the center-of-mass and rotational diffusivity of an isolated particle, respectively, and are given by $d_r = 3k_BT\ln(2A)/8\pi\mu L^3$ and $\mathbf{D} = k_BT\ln(2A)/8\pi\mu L(\mathbf{I}+\mathbf{pp})$. The Stokes equations couple the hydrodynamic disturbance with the particle density field through an orientationally averaged body force:

$$-\mu\nabla^2\mathbf{u} + \nabla p = \mathbf{F}_g\int c d\mathbf{p}. \tag{5}$$

For simplicity, we assume that a particle's center-of-mass moves like a fluid element, and that the disturbance field may be linearized on the scale of the particle length to evaluate its rotational motion. As boundary conditions, we impose a no-slip condition and no mean particle flux at each of the walls: $\mathbf{u}=0$ and $\int(U_{sx}c - D_{xx}c_{,x})d\mathbf{p}=0$ at $x=0,h$ [$\mathbf{U}_s$ is the particle sedimentation velocity, the second term on the right-hand side of Eq. (2)]. To evaluate the stability of the above equations, we introduce a density perturbation in the wall-normal direction of the form $c = n\Psi(\mathbf{p}) + n\delta\tilde{c}(x,t,\mathbf{p})$, where Ψ is the orientational distribution function for a spatially homogeneous suspension (assuming negligible alignment effects near the wall). Ψ satisfies Eq. (4) for $\mathbf{u}=0$, and is given for a suspension with particle torque $\mathbf{T}=\mathbf{p}\times\hat{\mathbf{B}}$ as

$$\Psi = \frac{F\,\mathrm{Pe}_g}{4\pi\sinh(F\,\mathrm{Pe}_g)} e^{F\,\mathrm{Pe}_g\hat{\mathbf{B}}/|\hat{\mathbf{B}}|\cdot\mathbf{p}}. \tag{6}$$

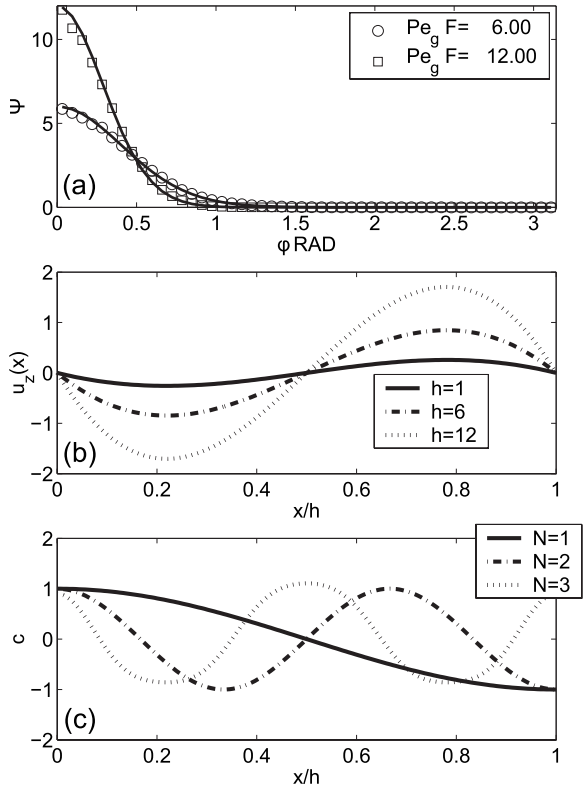

FIG. 1. (a) Concentration distributions at equilibrium using BDS and from the concentration equation solution. (b) The velocity disturbance in the direction of gravity for the most unstable eigenmode. (c) The first few unstable eigenmodes, in increasing order of stability for $h=12$ particle half lengths. All panels use $8nL^3=1$ and $A=20$.

Figure 1 shows the base state orientation distributions obtained from solving Eq. (4) for a homogeneous suspension compared to the distribution obtained from Brownian dynamics simulation of individual particles. BDS were performed at a dimensionless concentration of $8nL^3=0.6$, where n is the particle number density. The close agreement suggests the mean field yields a reasonable approximation to the real particle distributions.

To solve for the unknown perturbation function $\tilde{c}(x,t,\mathbf{p})$ to $O(\delta)$ and at different values of Pe_g and F, we expand $\tilde{c}$ in the spherical harmonics, which form a complete basis on the unit sphere: $\tilde{c} = \Sigma\Sigma b_{qs}(t,x)Y_{qs}(\mathbf{p})$ $(q=0\cdots\infty,\ s=-q\cdots q)$. It can be shown that to satisfy the no net particle flux boundary condition, the coefficients $b_{2,1}$ and $b_{2,-1}$ may be expanded in

a sine series, while the remaining coefficients may be expanded in a cosine series, i.e., $b_{qs}=\Sigma b_{qsm}(t)\cos(m\pi x/h)$ $(m=1\cdots\infty)$. The disturbance flow, obtained by substituting the expansion in Eq. (5), only has contributions from the $q=0$, $s=0$ harmonic modes, and can be shown to be simply a superposition of cosines:

$$u_z = 2n\delta\sqrt{\pi}\sum_m b_{0,0,m}\frac{|\mathbf{F}_g|h^2}{\mu(\pi m)^2}\left\{1-\cos\left(\frac{m\pi}{h}x\right)+3\left(\frac{x}{h}\right)^2[1+\cos(m\pi)]-2\left(\frac{x}{h}\right)[2+\cos(m\pi)]\right\}.$$

Substituting the perturbation function into the particle conservation equation (4), multiplying by $Y_{q's'}\cos(m'\pi x/h)$, and integrating in x and $\mathbf{p}$ yields a linear system of differential equations describing the time evolution of the expansion coefficients: $\mathbf{b}_{,t}=\mathbf{A}\mathbf{b}$. The solutions to this equation set are written $\mathbf{b}\sim\exp(\omega t)$, where ω is an eigenvalue of the expansion matrix $\mathbf{A}$. The sign of the real part of each eigenvalue, ω, therefore determines the stability of each solution (one corresponding to each index q, s, and m), and the largest such eigenvalue determines the overall suspension stability.

To evaluate the results of the mean-field analysis, we have performed BDS on sedimenting suspensions as described by Hoffman and Shaqfeh [7]. Our simulations resolve individual fiber dynamics, hydrodynamic interactions between fibers, and near-field lubrication interactions. In addition, we have included the effect of no-slip side walls through the use of a two-wall Greens function as derived by Liron [11] to evaluate the fluid velocity disturbance between particles. In all cases, we have taken the direction of $\hat{\mathbf{B}}$ to be parallel to the direction of gravity.

In Fig. 2, we analyze the effect of particle torque at constant container width $h=25$. In the left panel, two instability growth rates vs dimensionless particle torque F curves are shown at $\mathrm{Pe}_g=200$ and 100. It is clear that for a given Peclet number, the effect of increasing the field strength is to monotonically decrease the growth rate of the instability by altering the particle orientation distribution to a more aligned state which has a lower growth rate. Additionally, increasing F increases the torques responsible for alignment relative to the instability driving force, retarding the destabilization mechanism. The remarkable feature of this plot is that the curves intersect at $F\sim 0.01$, which represents the crossover region of Brownian demixing. For $F>0.01$, decreasing the Peclet number from 200 to 100, which represents an increase in thermal energy, destabilizes the suspension relative to the $\mathrm{Pe}_g=200$ case; that is, the suspension with a higher thermal energy has a higher perturbation growth rate. This is a somewhat counterintuitive result because, as we have described above, decreases in the Peclet number and increases in F both stabilize the suspension *when evaluated separately*. It is precisely because the stabilization mechanisms of Brownian motion and particle torque counteract one another that a region of demixing is found. We therefore expect a destabilization to occur when the rotational velocity induced by the external field approximately balances the rotation velocity induced by thermal motion $|\dot{\mathbf{p}}^F|\sim|\dot{\mathbf{p}}^{Br}|$, or $F\,\mathrm{Pe}_g\sim O(1)$.

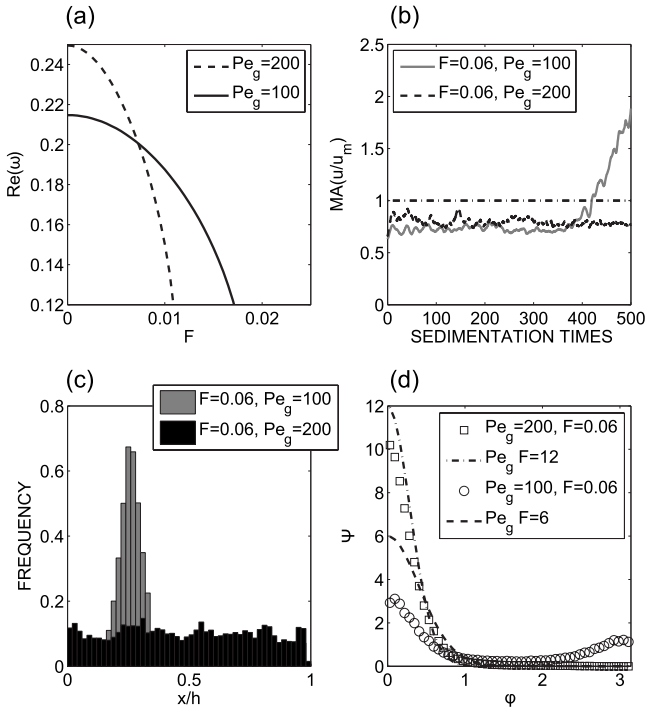

FIG. 2. (a) Mean-field analysis growth rates vs dimensionless torque. (b) Mean sedimentation velocity from BDS. (c) Cross-channel concentration profiles for a stable and unstable suspension. (d) BDS orientation distributions for a stable and unstable suspension. All panels at $8nL^3=0.25$.

Figures 2(b) and 2(c) show BDS results at constant F and two different Peclet numbers. After 400 sedimentation times, proportional to the time required for a rod to sediment its length $[t_s=8\pi\mu L^2/|\mathbf{F}_g|\ln(2A)]$, an instability develops in the suspension with $\mathrm{Pe}_g=100$, while that at $\mathrm{Pe}_g=200$ remains stable (defining stability as a moving average of the mean sedimentation velocity which remains below the maximum value for an isolated particle). The stable suspension remains uniformly distributed in space [Fig. 2(c)] along the channel width and a dense streamer forms near $x/h=0.3$ in the unstable case. In the stable suspension, concentration perturbations are insufficient to overcome the aligning effects of the field and are dissipated by center-of-mass Brownian motion before they can amplify. After the instability forms at $\mathrm{Pe}_g=100$, the orientation distribution distorts significantly from that of the stable suspension [Fig. 2(d), Eq. (6)]. Apparently, hydrodynamic torques overwhelm the field effects and create significant alignment antiparallel to the torque, a metastable state in which the particles experience no orientational change. The strength of the field is sufficient, however, to prevent particles from aligning perpendicular to gravity for long time periods.

Next, we examine the case of the sedimenting suspension without a particle torque to isolate the effects of no-slip walls on stability. From the mean-field analysis we find that long wavelength perturbations which span the entire container are the most unstable. In the bottom panel of Fig. 1 we show the first three unstable eigenmodes in increasing order of stability. The wave forms found in the no torque case are nearly identical to those found over the range of F examined above.

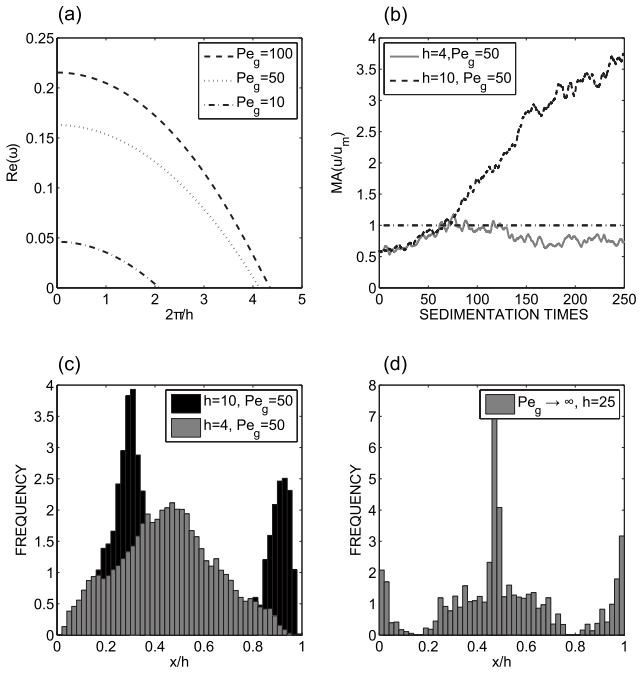

FIG. 3. (a) Growth rate of the longest wavelength concentration perturbation vs effective container wave number. (b) Mean sedimentation velocity as measured by BDS for $h=4$ and 10. (c) Mean cross-channel concentration profiles between 200 and 250 sedimentation times. (d) Cross-channel concentration profiles for a non-Brownian suspension. In all panels $8nL^3=1$.

In Fig. 1(b), the velocity disturbance in the direction of gravity is shown as a function of the channel width for the $N=1$ eigenmode and various h. The velocity field is characterized by alternating regions of downflow and backflow so as to give no mean flow. It is clear that a decrease in wall separation leads to a subsequent decrease in the magnitude (although not the wave form) of the resulting velocity disturbance. The no-slip walls essentially bound the container velocity fluctuations, resulting in a decrease in the hydrodynamic forces driving the instability and thus its growth rate.

We present in Fig. 3 combined results from the mean-field analysis and BDS for the case of no particle torque. In the top-left panel, the eigenvalue corresponding to the longest wavelength $\tilde{c}$ is plotted vs an "effective wave number." The results are essentially identical to those from the periodic analysis [7], the smallest wave number (largest h) suspensions are the least stable and the instability growth rate monotonically decreases as the space separating the container walls decreases (keeping particle concentration constant). Decreasing the Peclet number also retards the instability growth rate as described above. In the remaining panels of Fig. 3, the mean sedimentation velocity (b) is plotted vs time as measured by BDS, as well as the concentration in the wall normal direction averaged between $t=200$ and 250. Clearly, decreasing the spacing between walls suppresses the growth rate. The suspension with $h=4$ remains stable (by our definition) over the course of the simulation, while that with $h=10$ forms a dense streamer centered approximately at $x/h=0.4$.

There is, however, a contrast in the wave form of the instability as compared to the mean-field analysis. Instead of a single streamer forming along a side wall, the streamer forms 4 particle lengths away; additionally, a second streamer forms near the right wall [Fig. 3(c)]. As the first streamer develops, the particles farthest away from the perturbation are trapped by the resulting backflow. Because they are unable to pass through the wall, a secondary streamer is formed. This concentration profile most resembles the $N=2$ concentration perturbation eigenfunction from Fig. 1, suggesting that the nonpenetrable walls may provide a wave-number selection mechanism. The results are also apparent when considering non-Brownian suspensions [Fig. 3(d)], where the $N=3$ wave form appears. A key feature from the BDS missing from the mean-field theory is the presence of a hydrodynamic wall drift [12], which may provide a wave-number selection mechanism. Although it is outside of the scope of this Rapid Communication, the effect of no-slip walls on wave-number selection deserves further study.

In summary, we have demonstrated that the phenomenon of Brownian demixing can occur in suspensions where particle orientations are influenced by a *general* torque and may be found in a wide variety of systems. Additionally, we find that no slip walls effectively bound velocity fluctuations and influence the growth rate of instability, a result especially important for microfluidic applications.

We would like to thank the Army High Performance Computing Center (AHPCRC) at Stanford as well as the National Science Foundation under Grant No. CBET-0729771 for funding.

[1] K. A. Rose, J. A. Meier, G. M. Dougherty, and J. G. Santiago, Phys. Rev. E **75**, 011503 (2007).
[2] N. Gottschlich, S. Jacobson, C. Culbertson, and J. Ramsey, Anal. Chem. **73**, 2669 (2001).
[3] S. Pennathur, F. Baldessari, J. Santiago, M. Kattah, J. Steinman, and P. Utz, Anal. Chem. **79**, 8316 (2007).
[4] P. G. Righetti, C. Gelfi, and M. R. D'Acunto, Electrophoresis **23**, 1361 (2002).
[5] D. Saintillan, E. Darve, and E. Shaqfeh, J. Fluid Mech. **553**, 347 (2006).
[6] B. Herzhaft and E. Guazzelli, J. Fluid Mech. **384**, 133 (1999).
[7] B. Hoffman and E. Shaqfeh, J. Fluid Mech. (to be published).
[8] D. Koch and E. Shaqfeh, J. Fluid Mech. **209**, 521 (1989).
[9] D. Santillan, E. Shaqfeh, and E. Darve, Phys. Fluids **18**, 121503 (2006).
[10] D. Saintillan, E. S. G. Shaqfeh, and E. Darve, Phys. Fluids **18**, 121701 (2006).
[11] N. Liron, J. Eng. Math. **30**, 267 (1996).
[12] J. R. Smart and D. T. Leighton, Phys. Fluids A **3**, 21 (1990).